Enhancement of Proton Conduction at Low Humidity by Incorporating Imidazole Microcapsules into Polymer Electrolyte Membranes

*Jingtao Wang, Xiujun Yue, Zizhuo Zhang, Zheng Yang, Yifan Li, Han Zhang, Xinlin Yang, Hong Wu, and Zhongyi Jiang**

Design and fabrication of hierarchically structured membranes with high proton conductivity is crucial to many energy-relevant applications including proton exchange membrane fuel cell (PEMFC). Here, a series of imidazole microcapsules (IMCs) with tunable imidazole group loading, shell thickness, and lumen size are synthesized and incorporated into a sulfonated poly(ether ether ketone) (SPEEK) matrix to prepare composite membranes. The IMCs play two roles: i) Improving water retention properties of the membrane. The IMCs, similar to the vacuoles in plant cells, can render membrane a stable water environment. The lumen of the IMCs acts as a water reservoir and the shell of IMCs can manipulate water release. ii) They form anhydrous proton transfer pathways and low energy barrier pathways for proton hopping, imparting an enhanced proton transfer via either a vehicle mechanism or Grotthuss mechanism. In particular, at the relative humidity (RH) as low as 20%, the composite membrane exhibits an ultralow proton conductivity decline and the proton conductivity is one to two orders of magnitude higher than that of SPEEK control membrane. The enhanced proton conductivity affords the composite membrane an elevated peak power density from 69.5 to 104.5 mW cm^{-2} in a single cell. Moreover, the application potential of the composite membrane for CO_2 capture is explored.

1. Introduction

Proton transfer plays pivotal role in diverse chemical/biological processes and technological devices such as PEMFC.[1–3] Within cell membrane, directional transfer of protons can create transmembrane electrochemical potential, which drives the production of adenosine triphosphate, the fuel of life. Likewise, within PEMFC, proton transfer from anode to cathode through proton exchange membrane (PEM) is indispensable to fulfill the conversion of chemical energy into electrical energy. It is well known that PEM is the central and often the performance-limiting part of PEMFC. Presently, Nafion is the dominant PEM material due to its high, selective permeability to water and proton. Nafion can achieve proton conductivity as high as 0.1 S cm^{-1} at hydrated conditions owing to the continuous, ordered nanochannels.[4,5] To increase fuel cell efficiency, facilitate heat and water management, and diminish catalyst poisoning, high temperature (>120 °C) and low humidity (<50% RH) are desired.[6,7] However, under such conditions, the proton conductivity of Nafion drops to below 10^{-3} S cm^{-1} for the severe water loss and nanochannel deformation.[8,9] Development of PEM with affordable proton conductivity in broad applications remains a daunting challenge.

Theoretically, proton transfer through PEM obeys vehicle mechanism and Grotthuss mechanism.[10,11] The former is related to the proton diffusing together with water by forming a complex such as H_3O^+, $H_5O_2^+$, and $H_9O_4^+$. The latter is related to the proton hopping from one proton carrier site to a neighboring one through hydrogen bonds. Accordingly, for enhancing the proton transfer by vehicle mechanism at low humidity, PEM should possess high water retention properties, that is, high water uptake as well as slow and controllable water loss. The dominant approach is to incorporate hygroscopic solid, porous, hollow inorganic/organic fillers into membrane bulk, which render additional hydrogen-bonding sites or water storage space.[12–15] For enhancing the transfer by Grotthuss mechanism at low humidity, the dominant approach is to introduce anhydrous proton carrier by using heterocycles, such as imidazole, triazole.[14–18] Imidazole group has two nitrogen atoms, in which one nitrogen atom accepts a proton while the other nitrogen atom donates a proton. Proton transfer can occur with low reorientation and hydrogen-bond breaking/forming barriers, enabling anhydrous proton transfer via Grotthuss

Dr. J. Wang, X. Yue, Z. Zhang, Z. Yang, Y. Li, H. Wu, Prof. Z. Jiang
Key Laboratory for Green Chemical Technology
Ministry of Education
School of Chemical Engineering and Technology
Tianjin University
Tianjin 300072, China
E-mail: zhyjiang@tju.edu.cn
Dr. H. Zhang, Prof. X. Yang
Key Laboratory of Functional Polymer Materials
Ministry of Education
Institute of Polymer Chemistry
Nankai University
Tianjin 300071, China

DOI: 10.1002/adfm.201201436

mechanism. Coincidently, imidazole group is a common motif in biological proton transport in the form of histidine, and for example, protons are transported through imidazole group in M2 channel of influenza A virus with hundreds of microsecond.[19] Moreover, in many biological systems, imidazole group is utilized to manipulate water to be either trigonally distorted or tetrahedrally distorted.[20] In such a way, water can form continuous water networks for proton hopping. Since Grotthuss mechanism relies on a short-distance proton hopping (<0.275 nm), the imidazole group amount should be high enough to form continuous pathway for facile proton transfer.[21] It is reported that proton conductivity of free imidazole-bearing membranes increases over ten times with imidazole amount increasing from 0 to 80 wt%.[22,23] Since imidazole is in free form, these membranes often suffer from the imidazole loss, which causes Pt poisoning during operation. Anchoring imidazole group onto polymer chains or inorganic fillers is a feasible solution.[24,25] However,–NH group of imidazole group is usually protected by benzylation to avoid the lone pair electrons participating nucleophilic substitution reaction, which increases the steric hindrance of grafting reaction, and causes low grafting degree and imidazole group amount (<10 wt%).[24,26,27] In the present study, for the first time, imidazole polymeric microcapsules (IMCs) with high imidazole group loading and large lumen are designed and synthesized. The IMCs are then incorporated into SPEEK membrane to prepare the composite membranes. The IMCs play the following multiple roles: the lumen of IMCs acts as the water reservoir, the shell of IMCs manipulates the water release, mimicking the water storage mechanisms in plant cell and endowing an improved water retention properties; the imidazole group on IMCs shell renders anhydrous proton carrier pathways, imparting an enhanced proton transfer via either vehicle mechanism or Grotthuss mechanism; concomitantly, acid-base pairs are formed between sulfonic acid group on SPEEK and imidazole group on IMCs, mimicking the Schiff base-aspartic acid complex in bacteriorhodopsin (bR),[28] further facilitating the proton transfer.

2. Results and Discussion

2.1. Synthesis of Imidazole Microcapsules

Imidazole microcapsules are synthesized via selective removal of silica core from silica/poly(ethylene glycol dimethacrylate-*co*-vinylimidazole) (silica/P(EGDMA-*co*-VI)) microspheres via distillation–precipitation polymerization. This approach is chosen because the functional monomer (VI) and crosslinker (EGDMA) can be facilely radically copolymerized without protection and de-protection steps to coat the silica template via a vinyl capture process, and imidazole group loading is finely tuned via the VI/EGDMA ratio. The lumen size and shell thickness of IMCs are tuned by adjusting the silica core size and polymerization cycle/times. Roughly, IMCs with three kinds of imidazole group loading amount (31, 42, 59 wt%), three kinds of lumen size (180, 410, 620 nm), and three kinds of shell thickness (110, 150, 200 nm) are synthesized (**Table 1** and **Figure 1**). Fourier transform infrared (FTIR) spectra (Figure 1d) show that the IMCs display the characteristic peaks of imidazole at 3145 and 1640 cm^{-1} corresponding to the stretching vibration of –N-H and heteroaromatic ring, respectively. It should be noted that the imidazole group loading amount up to 59 wt% in our study, may be the highest among the analogous materials.[24–27] Imidazole microspheres (IMSs, 0#) with diameter of 610 nm as analogy of 2# are also synthesized. The zeta potential values of these IMCs and IMSs probed by ZetaPALS range from +7.7 to +8.6 mV, indicating the partial protonation of imidazole group and positively charged surface of IMCs and IMSs.

Table 1. The lumen size, shell thickness and imidazole group loading amount of the synthesized microspheres and microcapsules.

Sample	Lumen size [nm]	Shell thickness [nm]	Imidazole group loading amount [wt%]
0#	0	610 ± 10	41.7
1#	180 ± 2	110 ± 4	43.1
2#	410 ± 3	105 ± 2	47.5
3#	620 ± 4	110 ± 3	43.4
4#	410 ± 3	150 ± 3	42.3
5#	410 ± 3	200 ± 2	43.0
6#	410 ± 3	105 ± 8	30.7
7#	410 ± 3	102 ± 4	58.7

2.2. Characterization of the Membranes

The IMCs and IMSs are embedded into SPEEK matrix to prepare composite membranes via solution casting method. Field emission scanning electron microscope (FESEM) images reveal that the IMCs retain the pristine structure and disperse evenly within SPEEK bulk (Figure 1f). During freeze-fracture in liquid nitrogen, the IMCs are partially broken and their large lumens can be clearly observed at the cross-section of composite membrane. FTIR spectra of composite membranes are shown in **Figure 2**a. The major vibration peaks associated with the O=S=O of SPEEK control membrane at 1022, 1078, and 1225 cm^{-1} are found in all the composite membranes,[29] but the intensities decrease upon IMCs incorporation, which is probably due to the formation of S=O···H-N–hydrogen bonds between IMCs and SPEEK. Compared with SPEEK control membrane, the composite membranes exhibit higher peak intensity at 1650 cm^{-1}, attributed to the vibration of heteroaromatic ring in IMCs. In addition, a new peak appears at 1109 cm^{-1} (dashed line in Figure 2a), which is assigned to the symmetric stretching of $–SO_3^-$ and is an indication that the –S-OH group of SPEEK is deprotonated to generate –S-O^- group in the presence of IMCs.[30] The deprotonated protons would protonate the nitrogen atoms of imidazole group, yielding the attractive interactions between IMCs and SPEEK in the form of –S-O^-···$^+$H-HN– and –S-O^-···$^+$H-N =.[31] In such a manner, sulfonic acid-imidazole pairs (acid-base pairs) emerge at IMCs-SPEEK interface.

The embedment of IMCs in the membranes alters polymer chain mobility as reflected by glass transition temperature (T_g, Figure 2b). SPEEK control membrane displays a T_g of 162.4 °C,

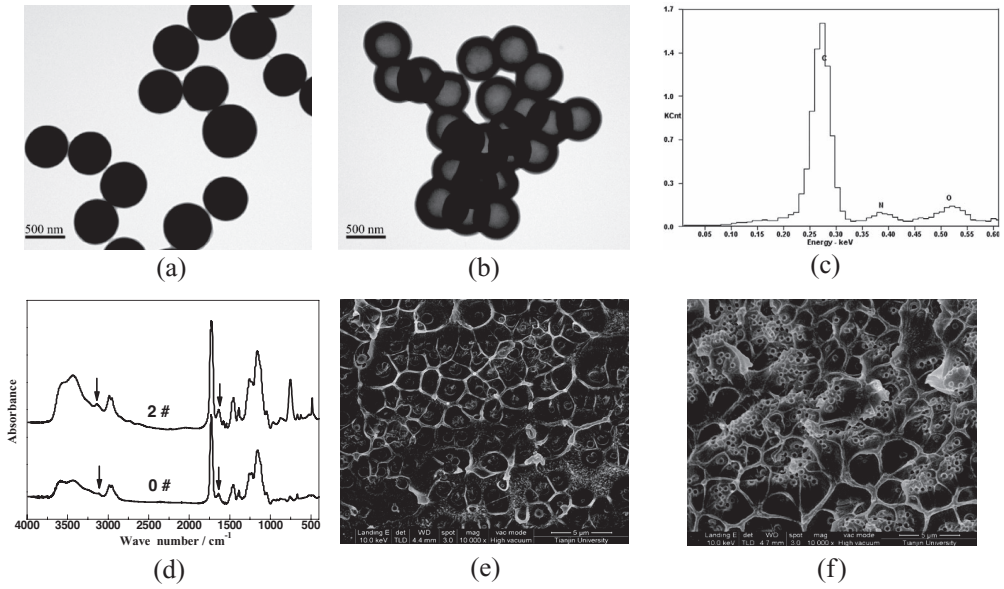

Figure 1. TEM images of a) imidazole microspheres (0#) and b) microcapsules (2#). c) EDS curve of the imidazole microspheres. d) FTIR curves of the imidazole microspheres and microspheres. FESEM images of the cross-section of e) SPEEK/0#-10 and f) SPEEK/2#-10 membranes.

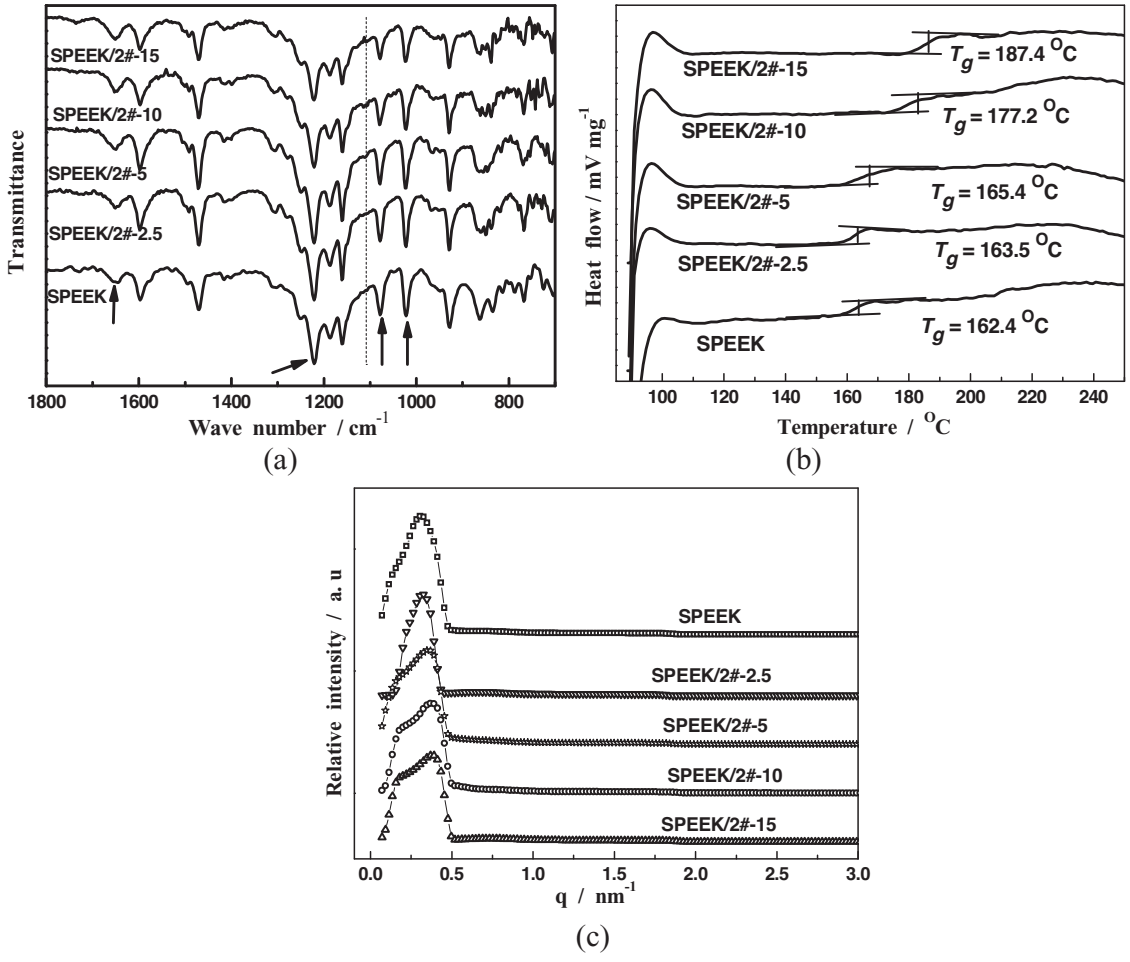

Figure 2. a) FTIR, b) DSC, and c) SAXS curves of SPEEK control and SPEEK/IMCs composite membranes. The degree of sulfonation of SPEEK is 0.66.

which is close to the literature results.[32] The composite membranes with the IMCs content of 2.5, 5, 10, and 15 wt% acquire the T_g of 163.5, 165.4, 177.2, and 187.4 °C, respectively. The increase in T_g further verifies the formation of electrostatic attraction between IMCs and SPEEK, which hinders the SPEEK chain mobility, thus requiring a higher activation energy for the identical motion state. The small-angle X-ray scattering (SAXS, Figure 2c) shows a typical scattering peak at q of around 0.3 nm^{-1} for all the membranes, indicating the existence of ionic nanochannels,[33] which result from the phase separation between hydrophobic and hydrophilic domains of SPEEK matrix. IMCs incorporation may weaken the entropic driving force for phase separation through the electrostatic interactions, which in turn decreases the nanochannel size of composite membranes. Consequently, the composite membranes display higher q values (up to 0.38 nm^{-1}) of scattering peak compared with SPEEK control membrane (0.31 nm^{-1}). As the IMCs content increases, the electrostatic interactions become stronger, resulting in smaller nanochannels as reflected by a continuous increase of q value. Thermogravimetric analysis (TGA) measurement reveals that all the membranes are thermally stable up to 230 °C, which should meet the requirement for practical application of fuel cells.

2.3. Water Retention Properties of the Imidazole Microcapsules and Membranes

Water retention properties in terms of water uptake, water state, and water retention of the IMCs and IMCs-filled membranes are sensitive to the structure of IMCs. The IMCs (2#) which have the diameter close to IMSs (0#) but with a 410 nm lumen, exhibit a water uptake of 186.1%, 3.4 times of that of IMSs (54.3%, Table S1), showing the striking advantage of capsular structure for water storage like plant cell. For the IMCs with similar shell thickness, varying the lumen size from 180 (1#) to 620 nm (3#) makes an increase of water uptake from 132.2 to 204.8%. For the IMCs with similar lumen size, the water uptake decreases from 186.1 to 148.1% with the shell thickness increasing from 105 (2#) to 200 nm (5#). Incorporating IMCs elevates the water uptake from 38.4% for SPEEK control membrane up to 62.1% for composite membrane (Table S1, Supporting Information), hinting that the IMCs with high water uptake act as water reservoirs within SPEEK matrix, donating large space for water storage. The water uptake of IMCs directly governs the water uptake of IMCs-filled composite membrane i.e., the higher water uptake of IMCs would confer the higher water uptake to composite membrane.

Water state data of hydrated IMCs shown in Table S1 are derived from differential scanning calorimetry (DSC) measurement (**Figure 3**a). The bound water content in 1#, 2#, and 3# (with similar shell thickness) spans from 33.5 to 40.0% with the increase of lumen size, whereas the free water content remarkably increases from 98.7% for 1# to 164.8% for 3#. This phenomenon indicates that free water in hydrated IMCs is mostly from the lumen while bound water is mostly from the shell, wherein water molecules interact with nitrogen atoms of imidazole group to form hydrogen bond networks.[20] For 2#, 4#,

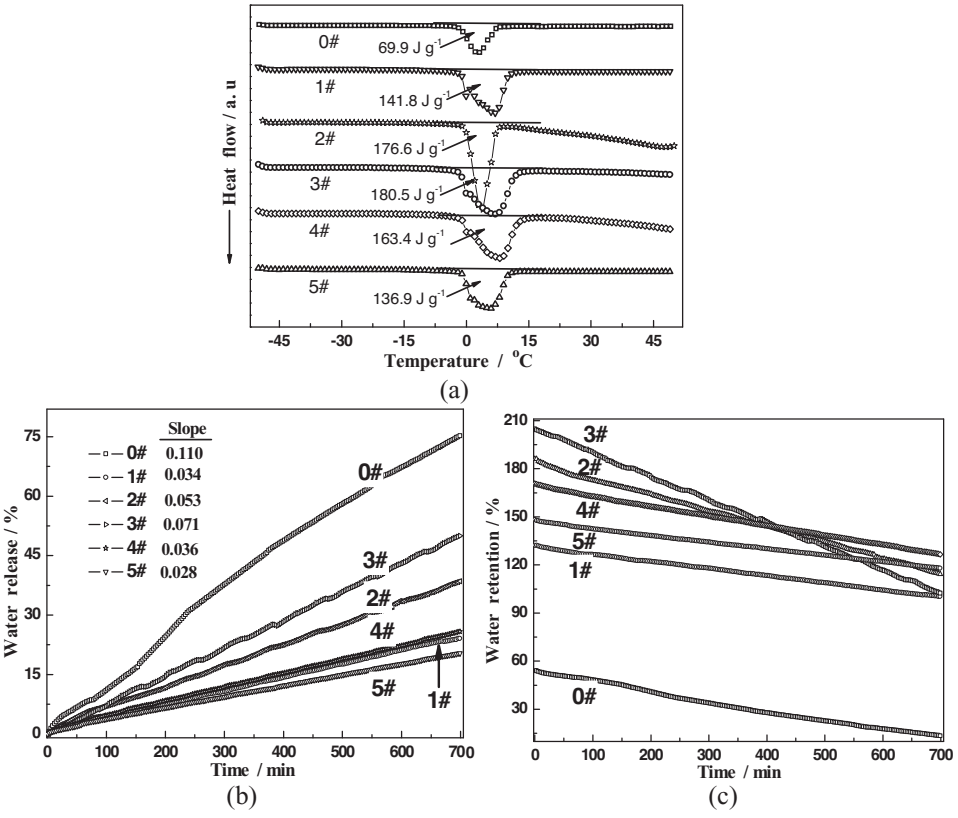

Figure 3. a) DSC thermograms, b) water release, and c) water retention of the imidazole microspheres and microcapsules as a function of time under 40 °C and 20% RH.

and 5# with similar lumen size but different shell thickness, the free water content decreases from 149.3% for 2# to 104.7% for 5#. For hydrated membrane, incorporating IMCs increases both free water and bound water amount. For instance, the free water content of composite membrane increases from 14.6% to 34.8% and the bound water content increases from 23.8 to 30.1%, when 15 wt% 2# is incorporated.

The dynamic water retention under low humidity is another crucial contributor. In this study, IMCs have ten times higher water retention than IMSs under 40 °C and 20% RH with lower water release rate (Figure 3), owing to the reduced chemical potential of sorbed water and switchable water state, resembling the water–retention mechanism in plants.[15,34] For IMCs with similar shell thickness (1#, 2#, 3#), larger lumen can render higher water storage capacity yet the faster water loss, yielding the slope of water release curve increasing from 0.034 (1#) to 0.071 (3#). When water is stored within a confined space, its vapor pressure obeys Kelvin and Young-Laplace equations.[35] Accordingly, larger lumen would increase the vapor pressure and hence the chemical potential of water within IMCs. Shell thickness exerts similar effects: thinner polymer shell endows higher water storage capacity but the faster water loss due to the shorter diffusion pathway and hence the less resistance for water diffusion. Collectively, the microcapsules should have moderate lumen size and shell thickness for optimum water retention properties. For SPEEK control membrane, water retention is 38.4% at beginning and reduces to below 2% after 180 min testing (**Figure 4**). Under identical conditions, up to 16.7% of water retention is obtained for SPEEK/2#-15. Moreover, the IMCs incorporation smoothes water retention curves of composite membranes, corroborating that the IMCs can supplement water into SPEEK matrix in a controlled way during water evaporation from the membrane. The other IMCs play the similar function.

2.4. Proton Conduction in the Membranes

Figure 5 depicts the proton conductivity of the membrane under 100% RH. The proton conductivities of SPEEK control membranes with degree of sulfonation (DS) of 0.56, 0.66, 0.75 are 0.011, 0.016, and 0.020 S cm^{-1}, respectively. In comparison, incorporating IMCs facilitates the proton transfer, yielding a conductivity about 0.021 S cm^{-1} (for SPEEK (DS 0.66)/6#). The notable increase in proton conductivity can be interpreted as follows: the IMCs promotes water uptake in the membrane, which facilitates proton transfer via vehicle mechanism by increasing proton-transport vehicles and dissociating proton donors (e.g., $-SO_3H$); meanwhile, sulfonic acid-imidazole acid-base pairs offer low energy barrier pathways for proton transfer. To verify the latter hypothesis, the proton conductivity of composite membrane with different sulfonic acid/imidazole ratios is tested. Varying the imidazole group loading amount of IMCs from 30.7 to 58.7 wt% results in an increase of proton conductivity of the composite membrane (DS of SPEEK 0.66) from 0.021 to 0.031 S cm^{-1}, much higher than that of pure

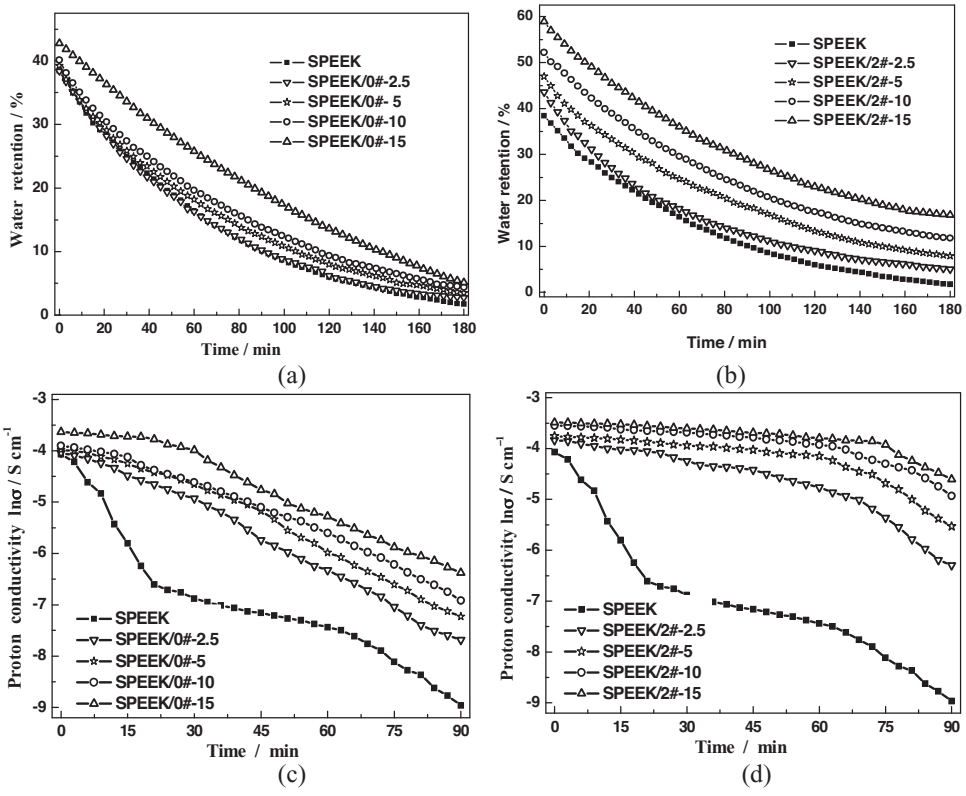

Figure 4. a,b) Water retention of the membranes as a function of time at 40 °C and 20% RH. c,d) Time dependence of proton conductivity of the membranes under 40 °C and 20% RH. The degree of sulfonation of SPEEK is 0.66.

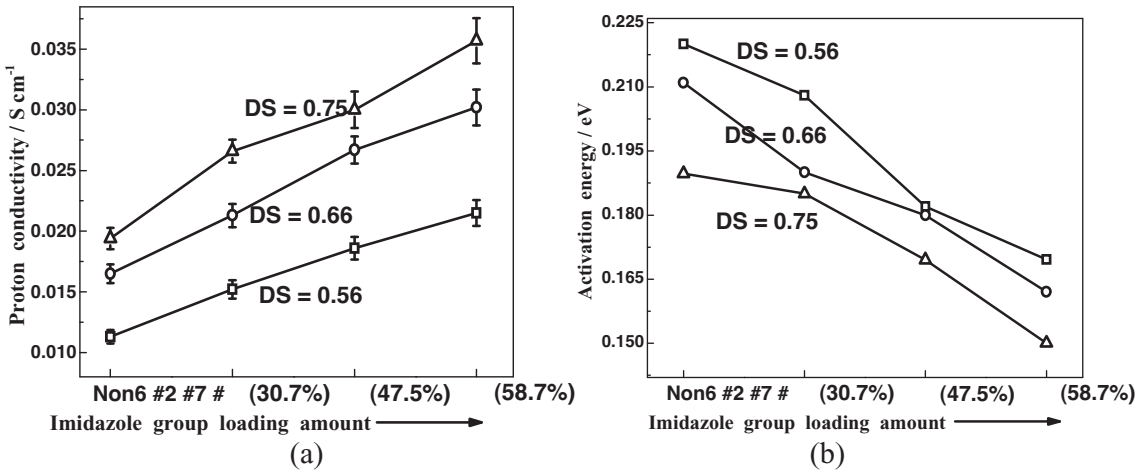

Figure 5. a) Proton conductivity at 30 °C and 100% RH and b) activation energy for proton transfer of SPEEK/IMCs composite membranes with different sulfonic acid/imidazole ratios. IMCs:SPEEK weight ratio is 10.0% for all the membranes.

imidazole molecules (<10^{-3} S cm^{-1}). Such results reveal the unique proton transfer feature of acid-base pairs, in which proton donor and acceptor are closely linked and protonation/deprotonation of one group is enhanced by the electrostatic attraction of the other group.[36] This electrostatic attraction also induces an optimum arrayed orientation of water networks for proton hopping. Similarly, increasing the DS of SPEEK affords an enhancement in proton conductivity of composite membrane. These findings suggest that increasing sulfonic acid and/or imidazole group amount can form more transfer pathways, resulting in an increase of proton conductivity.[17c,37,38] The transfer barriering property through acid-base pairs is reflected by the activation energy (*Ea*) of conductivity. Compared with SPEEK control membrane, the presence of acid-base pairs dramatically reduces the *Ea* of composite membranes, and the *Ea* further decreases with increasing acid-base pairs. The reduced *Ea* and enhanced proton conductivity infer that the pathways created by acid–base pairs can ensure ultrafast proton conduction with low energy barrier.

Figure 4 shows the dynamic proton conductivity of the membrane under 20% RH, which reveals that the proton conductivity of SPEEK control membrane (DS 0.66) is initially 1.6×10^{-2} S cm^{-1} and reduces to 1.3×10^{-4} S cm^{-1} at 90 min (Figure 4c), with a reduction of 99%. This is due to the marked water loss (Figure 4a), which leads to shrinkage and disconnection of the nanochannels available for proton transfer. Under identical conditions, the proton conductivity decreases from 2.6×10^{-2} to 1.6×10^{-3} S cm^{-1} when 15 wt% IMSs is added into membrane. This value is surprising high when considering that the water retention behaviors of IMSs-filled membranes are close to that of SPEEK control membrane (Figure 4a). This conductivity behavior indicates a weak dependence of proton transfer on water retention, which is interpreted as follows: i) the IMSs incorporation increases the bound water amount in membranes, which ensures continuous water networks, and ii) amphoteric imidazole group can allow anhydrous proton carrier site. Protons are therefore transported via Grotthuss mechanism efficiently. Encouragingly, the proton conductivity of SPEEK/2#-15 keeps as high as 3.1×10^{-2} S cm^{-1} within the first 75 min, and decreases to 4.2×10^{-3} S cm^{-1} at the time of 90 min, in accordance with its high water retention as shown in Figure 4b. A similar phenomenon is observed for other IMCs-filled membranes. This is because the microcapsules, similar to the vacuoles in plant cell,[39] could release water into SPEEK matrix in a controllable way to deter the water loss within polymer matrix and thus render membrane a stable water environment. The bound water will stabilize the 3D structure of the nanochannels by minimizing the potential energy surface. Meanwhile, protons can transfer along imidazole-based pathways with weak water dependence. Persuasively, over ten times increase in proton conductivity is acquired by embedding imidazole microcapsules.

2.5. PEMFC Performances and CO_2 Capture Properties of the Membranes

As one of the key parts of fuel cell, PEM must have high proton conductivity for high fuel cell performance. **Figure 6**a shows single cell performances using the as-prepared membranes with humidified H_2/O_2 at T_{cell} = 60 °C. Compared with SPEEK control membrane (69.5 mW cm^{-2}), the cell performances of the composite membranes are much higher. The peak power densities of single cell using SPEEK/0#-10 and SPEEK/2#-10 are 92.4 and 104.5 mW cm^{-2}, respectively. The elevated performances are partly originated from the enhanced proton conductivity of composite membranes, which promotes the reduction reaction in the cathode of fuel cell. For composite membrane, the microcapsule–filled membrane exhibits higher output performances than the microsphere–filled membrane owing to the higher proton conductivity. Meanwhile, incorporating IMCs yields a lower activation loss and ohmic loss of the fuel cell. For instance, the SPEEK/2#-10 has a maximum power density of 104.5 mW cm^{-2} at 0.38 V, whereas the SPEEK control membrane has 69.5 mW cm^{-2} at 0.33 V. The increased performances hint that the Pt poisoning by imidazole is substantially inhibited.

CO_2 as the main component of the greenhouse gases, its accumulation in the environment is leading to severe global warming

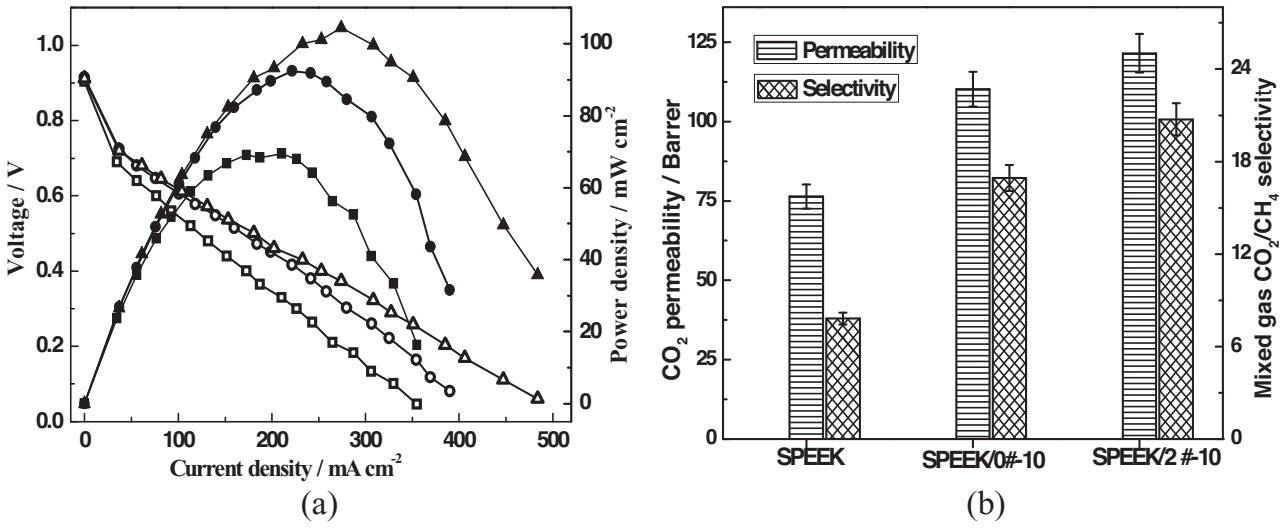

Figure 6. a) Single cell performances of the membrane with humidified H_2/O_2 operated at 60 °C (rectangle: SPEEK, circle: SPEEK/0#-10, triangle: SPEEK/2#-10). b) Mixed gas CO_2/CH_4 (10/90, vol/vol) selectivity and CO_2 permeability of the membrane at 25 °C. The feed pressure was 2 bar and feed flux rate was 150 cm^3 min^{-1}. The degree of sulfonation of SPEEK was 0.66.

issues, and CO_2 capture is of great interest and urgent need. CO_2 is an impurity in many natural gas wells, and it must be removed to ensure the energy content and avoid corrosion in the presence of water.[40] The potential of the composite membranes for CO_2 capture is explored (Figure 6b). SPEEK control membrane displays a typical CO_2 permeability of 76.4 Barrer and CO_2/CH_4 selectivity of 7.8. In comparison, the IMCs-bearing composite membrane wins a 59% increase in permeability (121.6 Barrer) along with a 165% increase in selectivity (20.7). The presence of IMCs notably enhances CO_2 adsorption capacity and creates additional pathways for CO_2 hopping through the basic nitrogen atoms of imidazole group. The additional pathways facilitate CO_2 diffusion while hardly affect CH_4 diffusion, the CO_2/CH_4 selectivity of composite membrane is enhanced accordingly. Under identical conditions, imidazole microspheres display similar function in elevating CO_2 permeability (110.2 Barrer) and selectivity (16.9) of the composite membrane.

3. Conclusions

In summary, we have developed a facile and generic approach to enhance the proton conductivity of proton exchange membrane under low humidity by incorporating imidazole microcapsules into SPEEK polymer bulk matrix. The imidazole microcapsules could render superior water retention property, unique anhydrous proton transfer pathway as well as sulfonic acid-imidazole acid-base pairs, thus conferring composite membranes up to 100 times increase in proton conductivity under 20% RH and a 51% increase in peak power density of single cell. Moreover, the composite membranes exhibit excellent separation performance for CO_2/CH_4 mixture, hinting their great application potential in CO_2 capture. The controlled water retention property, the anhydrous proton transfer pathway as well as the acid-base pair structure of as-prepared composite membranes guarantee their promising prospects in diverse energy and environment relevant fields.

4. Experimental Section

Synthesis of the IMCs and IMSs: 3-(Methacryloxy)propyltrimethoxysilane (MPS)-modified silica particles are synthesized by Stöber method.[15] A typical procedure for synthesizing silica/P(EGDMA-*co*-VI) microspheres is: MPS-modified silica (0.30 g), EGDMA (0.60 mL), VI (0.60 mL), and 2,2′-azobisisobutyronitrile (AIBN, 0.024 g) are dissolved in acetonitrile (80 mL) in a two-necked flask. The mixture is heated to boiling point. After half of acetonitrile is distilled out, the hybrid microspheres are purified. Core-shell hybrid microspheres are synthesized similar to the above procedure using the semi-batch mode as cores. Adjusting the cycle/times of polymerization process allows a desired thickness, and adjusting the VI/EGDMA ratio allows a controlled composition. The hybrid microspheres are etched in HF solution and followed by water washing. The final IMCs are obtained after drying. P(EGDMA-*co*-VI) microspheres (IMSs) are prepared by the similar process but without silica templating.

Preparation of Composite Membranes: A certain amount of IMCs or IMSs are dispersed into dimethylformamide (DMF, 12.0 g) under ultrasonic and stirring for 8 h. Then, SPEEK (1.20 g) is added into the DMF solution and stirred vigorously at room temperature for 24 h. The solution is cast onto a glass plate and dried overnight at 60 °C in a vacuum oven, and then at 80 °C for 8 h. The composite membrane is designated as SPEEK/M-X, where M represents the name of IMCs or IMSs, X represents the weight percentage of IMCs or IMSs to SPEEK.

Characterizations: Transmission electron microscopy (TEM) images are observed with a Tecnai G2 20 S-TWIN. The microstructure of the membranes is observed using FESEM (Nanosem 430) after being freeze-fractured in liquid nitrogen and then sputtered with gold. FTIR of sample is probed on a Nicolet MAGNA-IR 560 instrument with a resolution of 4 cm^{-1} in the range of 400–4000 cm^{-1} at room temperature. Glass transition temperature is obtained by DSC using a 204 F1 NETZSCH. Samples are preheated under nitrogen from room temperature to 150 °C at 10 °C min^{-1}, then cooled to 90 °C and reheated from that temperature to 260 °C. SAXS is carried out at a RigakuD/max2500v/Pc (Cu K 40 kV, 200 mv) in the range of 0.1–5.0°.

Measurement of Water Uptake and Water Retention: A dry sample (W_{dry}) is fully hydrated in water at constant temperature and then is weighed (W_{wet}). Water uptake is calculated by the equation: water uptake (%) = $(W_{wet}-W_{dry})/W_{dry} \times 100$. Immediately after water uptake measurement, the hydrated sample is set in a climate box to maintain 40 °C and 20% RH and is weighted ($W_{wet\ t}$) at time of t. Water retention is defined as

water retention (%) = $(W_{wet\,t}-W_{dry})/W_{dry} \times 100$. Water release is calculated by the equation: water release (%) = $(W_{wet}-W_{wet\,t})/(W_{wet}-W_{dry}) \times 100$.

Evaluation of Proton Conductivity, Single PEMFC, and CO_2 Capture: Proton conductivity of the membrane is measured in a conductivity cell by the AC impedance spectroscopy method. Membrane impedance is measured with a frequency response analyzer (FRA, Compactstat, IVIUM Tech.) with oscillating voltage of 20 mV over a frequency range of 1–10^6 Hz. The testing temperature is controlled by water vapor under a constant RH of 20% or 100%. The sample is hydrated in water for 48 h prior to measurement. Proton conductivity (σ, S cm^{-1}) is calculated from $\sigma = l/AR$, where l, A, and R denote the distance between the two probes, the cross-sectional area of membrane, and the membrane resistance, respectively. The membrane electrode assemblies (MEAs) with active area of 4 cm^2 are prepared by hot-pressing method at 140 °C and 4.0 MPa for 2 min. The loading of Pt catalyst is 0.10 and 0.25 mg cm^{-2} for anode and cathode, respectively. The PEMFC performances of MEAs are tested by using an in–house single fuel cell test set–up. The MEA is sandwiched between two graphite plates with flow channels. The single cell is operated at 60 °C with humidity H_2/O_2, and the humidification temperature is 60 °C. The flux rates of H_2 and O_2 are 150 and 200 ml min^{-1}, respectively. Prior to measurement, the cell is maintained under these experimental conditions for 4 h. Gas separation of CO_2/CH_4 (10/90, vol/vol) is conducted at 2 bar and 25 °C on a gas separation apparatus consisting of a stainless steel permeation cell. This cell exposes a hydrated membrane of 10 cm^2 to the gas. Feed gas and sweeping gas (N_2) flowrates are 150 cm^3(STP) min^{-1} and 80 cm^3(STP) min^{-1}, respectively. The composition of permeate is measured by a gas chromatography (Agilent 6820) equipped with a TCD detector.

Supporting Information

Supporting Information is available from the Wiley Online Library or from the author.

Acknowledgements

The authors gratefully acknowledge financial support from the National Science Fund for Distinguished Young Scholars (21125627), the National High Technology Research and Development Program of China (2012AA03A611), and the Program of Introducing Talents of Discipline to Universities (No. B06006).

Received: May 4, 2012
Revised: June 4, 2012
Published online: June 25, 2012

[1] B. P. Pedersen, M. J. Buch-Pedersen, J. P. Morth, M. G. Palmgren, P. Nissen, *Nature* **2007**, *450*, 1111.
[2] D. Riccardi, P. König, X. Prat-Resina, H. Yu, M. Elstner, T. Frauenheim, Q. Cui, *J. Am. Chem. Soc.* **2006**, *128*, 16302.
[3] Y. Chen, M. Thorn, S. Christensen, C. Versek, A. Poe, R. C. Hayward, R. T. Tuominen, S. Thayumanavan, *Nat. Chem.* **2010**, *2*, 503.
[4] R. Kannan, B. A. Kakade, V. K. Pillai, *Angew. Chem. Int. Ed.* **2008**, *47*, 2653.
[5] T. Tamura, H. Kawakami, *Nano Lett.* **2010**, *10*, 1324.
[6] J. Weber, K.-D. Kreuer, J. Maier, A. Thomas, *Adv. Mater.* **2008**, *20*, 2595.
[7] B. C. H. Steele, A. Heinzel, *Nature* **2001**, *414*, 345.
[8] S. Lu, D. Wang, S. P. Jiang, Y. Xiang, J. Lu, J. Zeng, *Adv. Mater.* **2010**, *22*, 971.
[9] N. Li, C. Wang, S. Y. Lee, C. H. Park, Y. M. Lee, M. D. Guiver, *Angew. Chem. Int. Ed.* **2011**, *50*, 9158.
[10] K.-D. Kreuer, *Chem. Mater.* **1996**, *8*, 610.
[11] T. J. Peckham, S. Holdcroft, *Adv. Mater.* **2010**, *22*, 4667.
[12] F. Pereira, K. Vallé, P. Belleville, A. Morin, S. Lambert, C. Sanchez, *Chem. Mater.* **2008**, *20*, 1710.
[13] K. Miyatake, T. Tombe, Y. Chikashige, H. Uchida, M. Watanabe, *Angew. Chem. Int. Ed.* **2007**, *46*, 6646.
[14] G. L. Athens, Y. Ein-Eli, B. F. Chmelka, *Adv. Mater.* **2007**, *19*, 2580.
[15] J. Wang, H. Zhang, X. Yang, S. Jiang, W. Lv, Z. Jiang, S. Z. Qiao, *Adv. Funct. Mater.* **2011**, *21*, 971.
[16] S. Bureekaew, S. Horike, M. Higuchi, M. Mizuno, T. Kawamura, D. Tanaka, N. Yanai, S. Kitagawa, *Nat. Mater.* **2009**, *8*, 831.
[17] a) K. D. Kreuer, A. Fuchs, M. Ise, M. Spaeth, J. Maier, *Electrochim. Acta* **1998**, *43*, 1281; b) W. Münch, K. D. Kreuer, W. Silvestri, J. Maier, G. Seifert, *Solid State Ionics* **2001**, *145*, 437; c) M. F. H. Schuster, W. H. Meyer, M. Schuster, K. D. Kreuer, *Chem. Mater.* **2004**, *16*, 329.
[18] C. A. Alabi, Z. Chen, Y. S. Yu, M. E. Davis, *Chem. Mater.* **2009**, *21*, 4645.
[19] M. Sharma, M. Yi, H. Dong, H. Qin, E. Peterson, D. D. Busath, H.-X. Zhou, T. A. Cross, *Science* **2010**, *330*, 509.
[20] L. E. Cheruzel, M. S. Pometurn, M. R. Cecil, M. S. Mashuta, R. J. Wittebort, R. M. Buchanan, *Angew. Chem.* **2003**, *115*, 5610.
[21] I. Presiado, J. Lal, E. Mamontov, A. I. Kolesnikov, D. Huppert, *J. Phys. Chem. C* **2011**, *115*, 10245.
[22] G. Lakshminarayana, R. Vijayaraghavan, M. Nogami, I. V. Kityk, *J. Electrochem. Soc.* **2011**, *158*, B376.
[23] M. Yamada, I. Honma, *Polymer* **2005**, *46*, 2986.
[24] Y. Lee, G. Scharfenberger, W. H. Meyer, G. Wegner, *Adv. Mater.* **2005**, *17*, 626.
[25] P. Mustarelli, E. Quartarone, S. Grandi, A. Carollo, A. Magistris, *Adv. Mater.* **2008**, *20*, 1339.
[26] G. Frutsaert, G. David, B. Ameduri, D. J. Jones, J. Rozière, X. Glipa, *J. Membr. Sci.* **2011**, *367*, 127.
[27] M. Schuster, W. H. Meyer, G. Wegner, H. G. Herz, M. Ise, M. Schuster, K. D. Kreuer, J. Maier, *Solid State Ionics* **2001**, *145*, 85.
[28] K. Faxén, G. Gilderson, P. Adelroth, P. Brzezinski, *Nature* **2005**, *437*, 286.
[29] H. Zhang, X. Li, C. Zhao, T. Fu, Y. Shi, H. Na, *J. Membr. Sci.* **2008**, *308*, 66.
[30] a) Z. Chai, C. Wang, H. Zhang, C. M. Doherty, B. P. Ladewig, A. J. Hill, H. Wang, *Adv. Funct. Mater.* **2010**, *20*, 4394; b) B. Bae, H. Y. Ha, D. Kim, *J. Electrochem. Soc.* **2005**, *152*, A1366.
[31] a) P. Totsatitpaisan, S. P. Nunes, K. Tashiro, S. Chirachanchai, *Solid State Ionics* **2009**, *180*, 738; b) J. Kerres, A. Ullrich, F. Meier, T. Häring, *Solid State Ionics* **1999**, *125*, 243.
[32] S. Swier, V. Ramani, J. M. Fenton, H. R. Kunz, M. T. Shaw, R. A. Weiss, *J. Membr. Sci.* **2005**, *256*, 122.
[33] a) K. Schmidt-Rohr, Q. Chen, *Nat. Mater.* **2008**, *7*, 75; b) A. Carbone, R. Pedicini, G. Portale, A. Longo, L. D'Ilario, E. Passalacqua, *J. Power Sources* **2006**, *163*, 18.
[34] M. T. Tyree, S. Yang, *Planta* **1990**, *182*, 420.
[35] a) M. J. Park, K. H. Downing, A. Jackson, *Nano Lett.* **2007**, *7*, 3547; b) S. Moghaddam, E. Pengwang, Y.-B. Jiang, A. R. Garcia, D. J. Burnett, C. J. Brinker, R. I. Masel, M. A. Shannon, *Nat. Nanotechnol.* **2010**, *5*, 230.
[36] O. F. Mohammed, D. Pines, E. T. J. Nibbering, E. Pines, *Angew. Chem. Int. Ed.* **2007**, *46*, 1458.
[37] Z. Zhou, S. Li, Y. Zhang, M. Liu, W. Li, *J. Am. Chem. Soc.* **2005**, *127*, 10824.
[38] M. Yamada, I. honma, *Angew. Chem. Int. Ed.* **2004**, *43*, 3688.
[39] C. Stock, H. K. Grønlien, R. D. Allen, Y. Naitoh, *J. Cell Sci.* **2002**, *115*, 2339.
[40] B. E. Gurkan, J. C. de la Fuente, E. M. Mindrup, L. E. Ficke, B. F. Goodrich, E. A. Price, W. F. Schneider, J. F. Brennecke, *J. Am. Chem. Soc.* **2010**, *132*, 2116.